

M. Dianat and I.P. Castro
 Department of Mechanical Engineering,
 University of Surrey,
 Guildford, U.K.

Abstract

In this paper we describe the application of pulsed-wire anemometry to the study of a two-dimensional separated flow generated by imposing a suitably adverse pressure gradient on a flat plate turbulent boundary layer. Accurate measurements of both mean velocity right down to the wall and skin friction have been made throughout the region approaching separation and within the separated region itself. The presentation includes a brief description of the development of the specially designed velocity probe which can be traversed through the wall and enables measurements to be made throughout the viscous dominated wall region. The data obtained within the separated boundary layer are compared briefly with the results of previous studies; in particular, the similarities and differences between shear layers bounding highly turbulent separated regions and the classic plane mixing layer are briefly discussed.

1. Introduction

The motivation for the present experiments has been to obtain a greater understanding of separated boundary layer flows. Perhaps the best known and best attested data for a flow of this sort are those of Simpson and his associates (Simpson et al¹). They used laser anemometry and were able to obtain reasonably accurate velocity and turbulence measurements throughout the whole flow, including the separated region itself. However, Simpson had no means of making skin friction measurements in this latter part of the flow so it is difficult to use the data to investigate the possibility of universal velocity profile shapes in the viscosity affected region near the wall. The basic objective of the present work was therefore to measure, as a first priority, velocity profiles and skin friction throughout the detachment and separated regions of a (nominally) two-dimensional separating boundary layer.

The method used to produce the required flow was similar to the one reported by Chu & Young², the details of which are given in the following Section. Flow adjustment with this arrangement appears to be somewhat easier than it is with Simpson's, in which a flexible tunnel roof was used. Section 2 also describes the measurement techniques used. The occurrence of a number of unexpected flow phenomena in the region prior to separation led to rather more measurements in that part of the flow than originally anticipated; these are discussed in Section 3. Section 4 presents some of the data obtained in the separated region and briefly discusses their implications.

2. Experimental Arrangements

2.1 The Wind Tunnel

The measurements were made in the blow-down, open circuit tunnel in the Department of Mechanical Engineering. Its working section is 0.76 x 0.61 x 4m long and the maximum velocity is around 17m/s.

At this speed the free stream turbulence level is below 0.25%. Figure 1 shows the experimental set-up used to produce the separating boundary layer. This is similar to the method used by Woodward³ who studied laminar separation bubbles. Later, Chu & Young² found this arrangement equally effective in producing turbulent boundary layer separation.

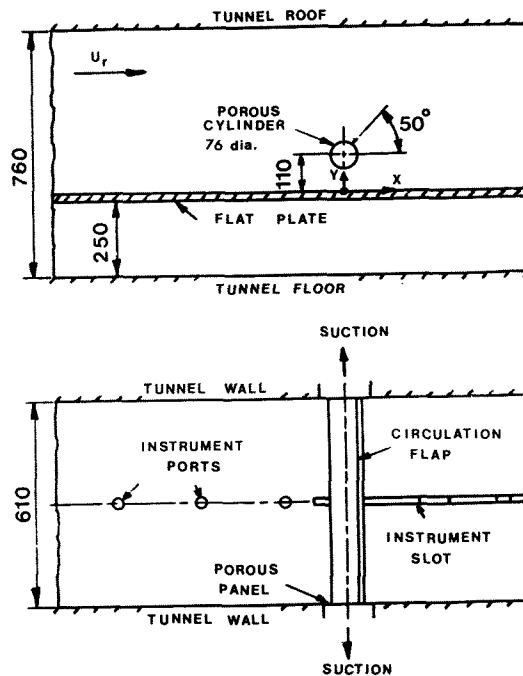


FIGURE 1. Experimental arrangements. Not to scale. Dimensions in mm.

The apparatus consisted of three aluminium flat plates, each 1.21m long and 10mm thick, which spanned the 0.6m horizontal width of the tunnel and formed the main 3.63m surface. An elliptical-nosed section was attached to the leading edge of the plate, which was at zero incidence and about 250mm above the floor of the tunnel. Two of the three sections of the flat plate were equipped with circular instrumentation ports positioned 200mm apart; the third, rearward section had a 0.84m slot fitted with segmented rectangular blocks of various lengths. For each measuring instrument a special block was constructed, with a suitable hole and appropriate probe fixing arrangements.

A porous cylinder of nominal diameter 75mm was mounted through the sidewalls of the tunnel about 110mm above the flat plate and normal to the flow. Its axis was parallel to the plate and about 2.7m from its leading edge. Attached flow was maintained around the cylinder by applying suction through the porous surface. A small flap fitted to the rear of the cylinder allowed generation of the required circulation - as the flap angle increased, more suction was required to maintain attached flow. Consequently the pressure gradient imposed

on the flat plate was initially favourable and then adverse. To prevent strong three-dimensional effects being generated by separations at the junction of the cylinder with the tunnel side-walls, the cylinder passed through porous circular discs set into the tunnel walls.

2.2 Measurement Techniques

For measuring the surface static pressure, 0.5mm diameter tappings in the instrumentation ports were connected to a calibrated capacitance transducer, whose output was averaged over, typically, 120secs. Some of the velocities in the regions of low turbulence level (less than 20%) were obtained using standard hot-wire anemometry and flattened pitot tubes. Preston tubes were used where appropriate for the measurement of skin friction. However, the major part of the study was undertaken using specially designed pulsed-wire wall skin friction and through-wall velocity probes, both of which were based on the time-of-flight technique originally described by Bradbury & Castro⁴.

Details of the skin friction probe and its potential and capabilities for measurements in three-dimensional highly turbulent flows are given in Castro & Dianat⁵ and Dianat & Castro⁶. It consists essentially of three fine wires about 2mm long mounted parallel to each other and 0.05mm above the surface. The sensor wires are of 5 micron tungsten and positioned 0.5mm either side of the central, 9 micron pulsed wire. All three wires are welded to prongs mounted in a 5mm diameter circular plug. The central wire is rapidly heated with a short electrical pulse and the time taken for the heat tracer to reach a sensor wire is measured. A separate probe of generally similar dimensions but with an increased spacing between the wires (1mm) was used in regions where the wall shear stresses were comparatively high.

The through-wall velocity probe has a geometry very similar to standard pulsed-wire probes but was constructed integral with a 16mm wall plug, so that the probe head could be traversed in and out using a micrometer beneath the surface of the plug. The pulsed wire was parallel to the surface and could be positioned between 0.025mm and 7mm from it, whilst the vertical sensor wires moved through small holes drilled through the surface. All wires moved together so that the overall geometry did not change with pulsed wire location. With this arrangement the calibration of the probe was independent of the particular position of the wires.

Both the skin friction and the velocity probes could be mounted in appropriate rectangular blocks or circular discs and positioned at any desired axial station, causing negligible flow disturbance. In both cases the instruments were interfaced to Commodore PET microcomputers, allowing on-line calibration and measurement.

2.3 Flow Adjustment

The suction applied to the cylinder surface was maintained at a fixed level by monitoring the suction pressure at one end of the cylinder. This was typically 250mm of water and was very close to the pressure at the other end, ensuring a good degree of suction uniformity along the cylinder

span. The suction required to maintain attached flow around the cylinder was determined by inspection of tufts attached on and either side of the flap; the minimum suction for which these remained steady was taken as the required value. No noticeable change in flow characteristics was observed for stronger suction. Traverses with a hot-wire anemometer showed that the cylinder wake was very thin and of low turbulent intensity (2% at most) at the height of the cylinder axis for the particular flap angle chosen.

There were some difficulties in obtaining the required flap angle. For an angle of, say, 35°, surface oil film visualisation revealed the presence of a clear separation line, but later measurements with the through wall probe showed that the separated region was much too thin for the purposes of the present study. Rows of tufts mounted on vertical 'strings' were therefore used downstream of the cylinder to observe the backflow region. This technique was found to be qualitatively very useful and a flap angle of 50° was finally chosen as one producing an adequate fully separated boundary layer.

The two-dimensionality of the flow was investigated by traversing single hot-wire and pulsed wire probes, where appropriate, across the span at various positions both within and outside the separated region. Careful setting up of the whole rig enabled a good degree of two-dimensionality and symmetry to be achieved over the central third of the span, with spanwise variations in mean velocity of no more than $\pm 1\%$ almost everywhere in the flow except near the separation line within the backflow region. As a further check, oil flow visualisation was undertaken in the vicinity of the separation line, which was found to be remarkable straight over practically the whole span. Just inside the backflow region, however, the flow tended to move sideways and outwards, with a weak saddle point close to the spanwise center-line.

Standard oil flow techniques were not very successful within the bulk of the separated region, where the method described by Langston & Boyle⁷ was applied. This further confirmed the two-dimensionality of the flow over the central third of the span. The position of the reattachment line was determined using the twin-tube probe described by Castro & Fackrell⁸. It was found to be straight to within $\pm 1.5\%$ of the length of the separated region (0.83m) over the central half of the span. Since the aspect ratio of the separated region (axial length/spanwise width) was only about 0.8 it seemed unlikely that the degree of two-dimensionality could have been significantly improved; it was thought to be quite adequate for the present purposes.

Figure 2 shows the static pressure distribution, plotted as a pressure coefficient, along the plate center-line. C_p is defined as $(p - p_r)/0.5\rho U_r^2$, where p_s is the surface pressure and suffix r refers to free stream conditions far upstream. It may be seen that a strong adverse pressure gradient follows an initial favourable distribution. After separation at $x=80\text{mm}$, where x is measured from the cylinder axis position, the pressure remains nearly constant before recovering to near its upstream value further downstream. Reattachment occurs at $x=910\text{mm}$. Note that neither

surface pressure nor flow velocity measurements have yet been made beyond $x = 750\text{mm}$.

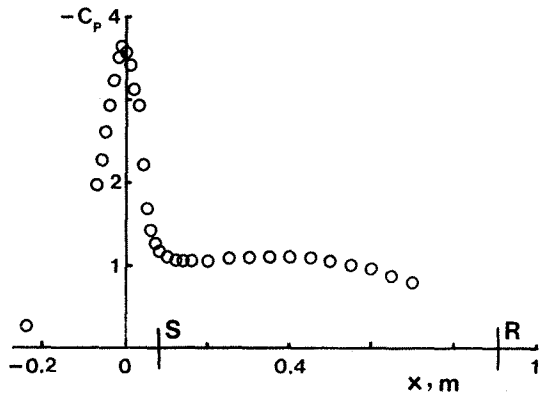


FIGURE 2. Surface static pressure distribution. S and R denote the locations of separation and reattachment, respectively.

3. The Flow Upstream of Separation

As an initial test, skin friction was measured throughout the flow. The wall probe was calibrated against Preston tubes in the 'standard' turbulent boundary layer far upstream of the cylinder (see Castro et al⁹ or Eaton et al¹⁰ for typical calibration details). The boundary layer was validated using Clauser log-law mean velocity plots, in addition to Preston tube measurements - Patel's¹¹ calibration was used for the latter.

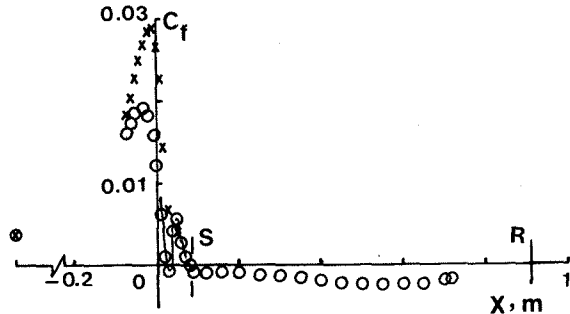


FIGURE 3. Skin friction distribution. O, pulsed wire; x, Preston tube.

Figure 3 shows the skin friction distribution throughout the flow, with the corresponding fluctuating data presented in Figure 4. (Here $C_f = \tau_w / 0.5\rho U^2$ and $c_f' = \sqrt{\tau_w^2} / 0.5\rho U^2$). Measurements obtained with a 1.48mm Preston tube are included in Figure 3. As expected, the flow experiences a continuous rise in skin friction due to the strong acceleration, followed by a sharp fall under the influence of the adverse pressure gradient. However, before the final separation the pulsed-wire wall probe indicates a rapid rise and subsequent fall in C_f . Preston tube data gives no indication of this behaviour; indeed, had the pulsed-wire probe not been used, we might have been entirely satisfied with the flow - the Preston tube results are very similar to those of Chu & Young². Closer investigation revealed that relaminarisation occurred in the highly accelerated region; this

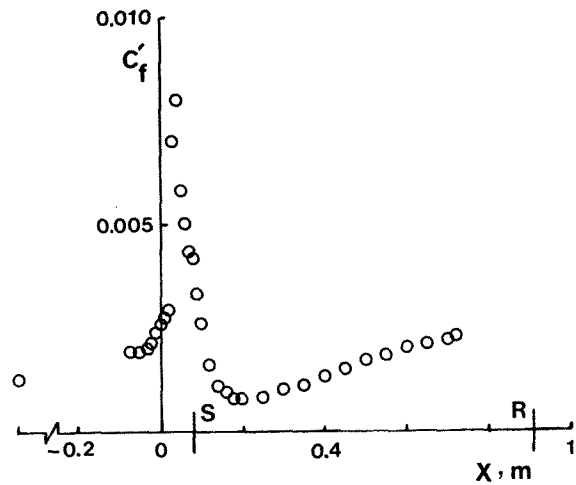


FIGURE 4. Fluctuating skin friction distribution.

persisted a short distance into the adverse pressure gradient region before transition to turbulence, with a consequent sudden rise in C_f , and finally turbulent separation at $x=80\text{mm}$. Note that c_f' falls to about 10% of C_f in the accelerated region, compared with its upstream value of about 30%. The latter is consistent with the near wall data of other investigators.

Now Kays et al¹² have suggested that if the 'acceleration parameter', $K = v/U_1^2 \cdot dU_1/dx$, where U_1 is the local free stream velocity, is maintained sufficiently large and constant along the flow the equilibrium value of the momentum thickness Reynolds number, Re_θ , can be below the critical Reynolds number for transition from laminar to turbulent boundary layer flow, in which case relaminarisation takes place. A common criterion for the critical value of K is $K > 10^{-6}$, beyond which 'laminar-like' behaviour is observed. If K exceeds 3×10^{-6} the entire boundary layer begins to relaminarise. This parameter is not readily available for the present experiments but, it may be estimated with reasonable accuracy from the surface pressure distribution and assuming that the pressure gradient normal to the surface is negligible. The calculation shows that K reaches a value as high as 6×10^{-6} , which is much higher than the above limit. Increasing the free stream velocity would reduce K (and increase Re_θ). However, in the present case a velocity of about 40m/s would be required to be certain of fully turbulent flow everywhere; this was not possible for various reasons. An alternative would be to reduce dC_p/dx by reducing the flap angle, but measurements showed that, firstly, the flow ceased to separate at smaller flap angles and, secondly, even for a zero angle only a modest reduction in K (to about 4×10^{-6}) was achieved. Further, pulsed wall probe measurements showed that the characteristic 'double hump' behaviour of C_f persisted even for this reduced value of K .

Despite this initial relaminarisation, it seemed likely that since the final separation was, in fact, a turbulent one, and the scale of the separated flow was so large, the nature of the latter would be largely independent of the details of the flow in the upstream region. As far as instrumentation is concerned, the fact that Preston tubes failed to capture the effects of relaminarisation should be regarded as a warning against its use in non-classical flows. Using log-

law fits to velocity data would be equally uncertain in the present case.

It is interesting here to analyse the data of Chu & Young², since they used an almost identical set-up. Because of a somewhat higher free stream velocity in their experiments (20m/s) the momentum thickness Reynolds number at the cylinder position but in its absence was about 4500, compared to 3000 in the present case. For the same reason their flow experiences a somewhat milder pressure gradient. However, the maximum value of K was in excess of 2×10^{-6} - lower than the present case but still above the critical value. There is a distinct possibility, therefore, that their flow had similar features to ours; perhaps they were not found because of instrumentation limitations. Note that in Simpson's experiments (Simpson et al¹) K is much lower, having a maximum value of about 3×10^{-7} .

A few velocity measurements made in the region prior to separation using the through-wall probe. This was calibrated at $x = -1.9m$ with the pulsed wire 7mm from the surface, where the turbulent intensity (in this outer region of the local boundary layer) was about 10%. An appropriate allowance for the turbulence was made, similar to that described by Eaton et al¹⁰.

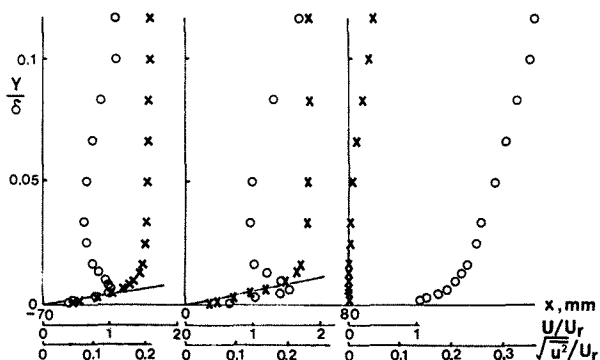


FIGURE 5. Mean velocity and turbulence intensity profiles prior to separation. x, mean velocity; O, intensity; —, velocity near the wall deduced from skin friction measurements.

Figure 5 shows the mean velocity and turbulent intensity profiles upstream of and at separation; the wall distance is normalised by the boundary layer thickness at the position of the cylinder but in its absence ($\delta = 60mm$). First, note that the velocity data asymptote to the gradient implied by the independent skin friction measurements as the wall is approached. This is a satisfying confirmation of the general consistency in the measurements. Second, at $x = -70mm$, turbulence intensities are generally low, about 13% of the mean velocity at most, confirming once again the laminar like behaviour in this region. Plots of mean velocity data in the usual wall-layer coordinates at $x = -70mm$ and $x = 0$ do not exhibit any clear linear region. This was expected - there is little reason to anticipate classic log-law behaviour near separation - but emphasises again the unsuitability of Preston tubes of any diameter.

4. The Separated Flow

The through-wall velocity probe was used in the region near the surface, whilst further away from the wall standard pulsed wire probes and, in the lower intensity regions, single hot wires were used. Figure 6 presents longitudinal mean velocity profiles at four stations after separation, with the wall distance normalised by the centre-line bubble length, L_r . Corresponding turbulence intensity profiles are shown in Figure 7.

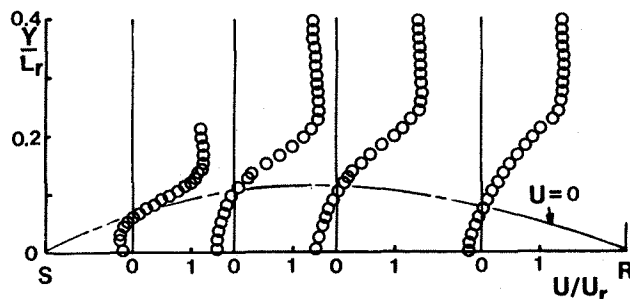


FIGURE 6. Mean velocity profiles in the separated flow. Note the locus of $U=0$.

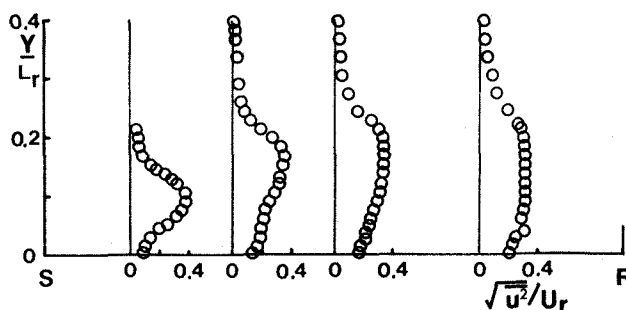


FIGURE 7. Turbulent intensity profiles in the separated flow.

The growth of the shear layer is commonly measured in terms of the increase in its vorticity thickness, Λ , defined by $\Lambda = \left| \frac{d(U/\Delta U)}{dy} \right|^{-1}_{max}$, where $\Delta U = U_1 - U_N$, U_1 and U_N being the maximum and minimum velocities, respectively. This is shown normalised by L_r and plotted against x'/L_r in Figure 8. x' is the distance from the separation point ($x' = x - 80mm$). The results of Ruderich & Fernholz¹³ (hereafter, RF), for the case of the separated region behind a normal flat plate with a long, central, downstream splitter plate, are included in the figure. Because of the limited number of velocity profiles obtained thus far it is not sensible to draw definitive conclusions, although it is interesting that the growth rate is apparently very similar to that of the classical plane mixing layer (PML), shown for comparison in the figure. However, the data of RF and some currently unpublicised data of our own in a similar flow is not really consistent with a linear increase in Λ . There is little reason to suppose that the shear layer bounding the reversed flow region in the present case should grow linearly.

Figure 9 shows the development of the maximum values of u^2 , normalised by $(\Delta U)^2$. The corresponding RF data is included, along with the value found in the PML. There are clear

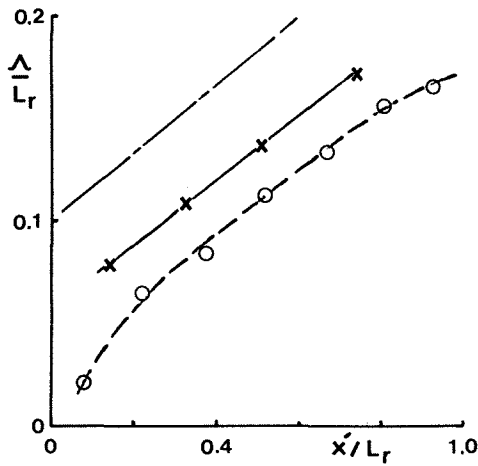


FIGURE 8. Growth of the vorticity thickness. x , present work; \circ , RF; ---, PML (arbitrary virtual origin).

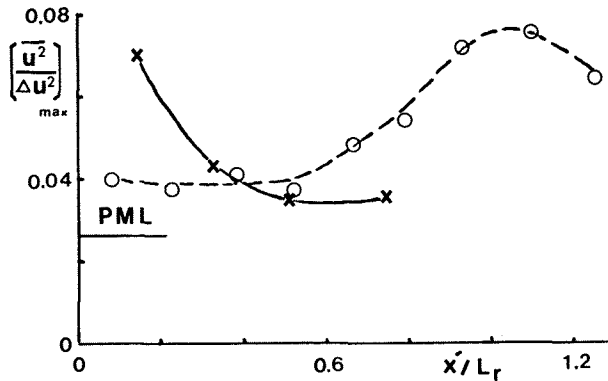


FIGURE 9. Development of the maximum normal Reynolds stress. Legend as in fig.8.

differences between these three cases, which are much more pronounced than the differences in growth rate. Indeed, the behaviour in the present case is qualitatively quite different from that found by RF in the normal flat plate flow. The latter shows a continuous rise towards reattachment and a fall thereafter; the present data has the opposite behaviour. This is probably caused by the unsteady nature of the separation in the present turbulent boundary layer flow. By 'unsteadiness' we mean here simply that the separation point is not fixed but fluctuates quite widely - instantaneous skin friction could take either sign over a range of axial distance spanning the time-mean $C_f = 0$ position, as has been shown by previous workers¹. Although the entire separated shear layer may well be influenced by this general unsteadiness, the effects might be anticipated to be more obvious in the region close to separation. Note that in the RF experiment the separation line was fixed at the sharp edge of the plate, so no corresponding unsteadiness occurred, although in our similar experiments there was some evidence of shear layer 'flapping'.

The trend in axial turbulence energy levels reverses in the region nearer the wall. This is evident from the results in figure 7 and is also demonstrated by the c_f' data shown in figure 4. It can be seen that c_f' is highest near the reattachment zone and decreases as the internal boundary in the separated region develops towards

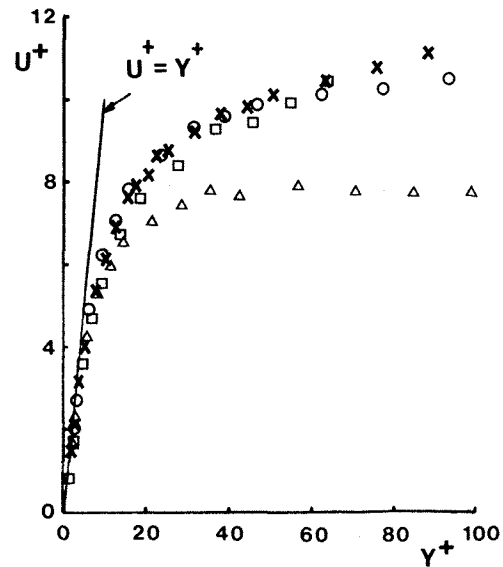


FIGURE 10. Backflow near-wall velocity profiles. x'/L_r : \square , 0.145; \times , 0.325; \circ , 0.506; \triangle , 0.747.

the separation point.

In the near wall region the flow must be significantly influenced by viscosity. Figure 10 presents the mean velocity data in this region, plotted in the usual wall units, using the wall shear velocity implied by the skin friction measurements. The profiles asymptote to the $U^+ = y^+$ line for $y^+ < 4$, again confirming the consistency of the measurements. Note, however, that the raw data (not shown) departed a little from this line in the sublayer region ($y^+ < 4$) - increasingly so as the wall was approached. This was due to the significant effects of diffusion in that region, which lead to a more complex heat tracer flight path. However, it was possible to apply corrections for these effects, based on simple ideas about the flight path. These corrections were validated in standard zero pressure gradient boundary layers and will be discussed in a forthcoming paper.

The U^+ vs. y^+ law-of-the-wall is not valid in the backflow region. This has been pointed out by Simpson et al¹, who found a good correlation when the mean velocity and distance from the wall were normalised by the maximum negative velocity, U_N and its distance from the wall, N , respectively. Figure 11 shows the data plotted in this form. Simpson¹⁴ suggested the use of:

$$U/U_N = A(y/N - \ln(y/N) - 1) - 1 \quad (1)$$

with $A=0.3$. In the present case a good correlation exists for $y/N < 1$ with $A=0.235$. The reason for this difference is not clear and further work is needed to substantiate the existence of a 'universal law'; it should be noted that Simpson's data showed considerably more scatter than is present in the results shown in figure 10.

The fact that this is a viscosity dominated region suggests the possibility of correlation between the friction coefficient and the Reynolds number if these are appropriately defined. Ignoring for the moment the highly turbulent nature of the backflow, one appropriate Reynolds number

5. Conclusions

With effective use of pulsed wire anemometry some new information about separating flows has been obtained. The major conclusions from this first phase of the work can be summarised as follows:

- 1) A separated shear layer bounding a highly turbulent reversed flow region has features quite different from those of the classical plane mixing layer. It seems further that these differences depend on the nature of the initial separation process.
- 2) The backflow mean velocity profile scales on the maximum negative mean velocity, U_N , and its distance from the wall, N , for $y/N < 1$ but the data differ somewhat from those of Simpson¹⁴, which were obtained in the separated flow following a rather milder adverse pressure gradient.
- 3) The flow close to the wall in the backflow region is strongly influenced by viscosity. Not only has the linear sub-layer been experimentally confirmed for $y^+ < 4$, but it seems that a universal collapse of skin friction data from separated flows of quite different geometry is possible.

Finally, it should be emphasised that the work described here forms just the first phase of an extensive investigation of separated boundary layer flows. We are currently undertaking a wide range of more detailed turbulence measurements, with the intention of making further comparisons between different kinds of separated flows and hence, hopefully, developing a deeper understanding of the reasons for differences between them.

6. Acknowledgements

The work would not have been possible without the technical skill of Mr. T. Laws in development of the pulsed wire probes. The financial support of the Procurement Executive, Ministry of Defence and the Science & Engineering Research Council, is also gratefully acknowledged.

7. References

1. Simpson RL, Chew YT & Shivaprasad BG. *J. Fluid Mech. (JFM)* **113**, 23 (1981).
2. Chu J & Young AD. AGARD CP-168, paper 13 (1976).
3. Woodward D. Ph.D Thesis, London (1970).
4. Bradbury LJS & Castro IP. *JFM*, **49**, 657 (1971).
5. Castro IP & Dianat M. *J. Wind Eng. Ind. Aero.* **11**, 107 (1983).
6. Dianat M & Castro IP. as above, **17**, 133 (1984).
7. Langston LS & Boyle MT. *JFM*, **125**, 53 (1982).
8. Castro IP & Fackrell JE. *J. Ind. Aero.* **3**, 1 (1978).
9. Castro IP, Dianat M & Bradbury LJ. To appear in 'Turbulent Shear Flows V', ed Durst et al. (1986).
10. Eaton JK & Johnston JP. Rep. MD-39, Thermo-Sciences Division, Dept. Mech. Eng, Stanford. (1980).
11. Patel VM. *JFM*, **23**, 185 (1965).
12. Kays WC & Crawford ME. *Convective Heat & Mass Transfer*, pp. 178-179, McGraw-Hill (1980).
13. Ruderich R & Fernholz HH. *JFM*, **163**, 283 (1986).
14. Simpson RL. *AIAA J.* **21**, 142 (1983).
15. Adams EW, Johnston JP & Eaton JK. Rep. MD-43, Mech. Eng. Dept., Stanford (1984).
16. Chandrsuda C & Bradshaw P. *JFM*, **110**, 171 (1981).
17. Devenport WJ. Ph.D Thesis, Cambridge (1985).

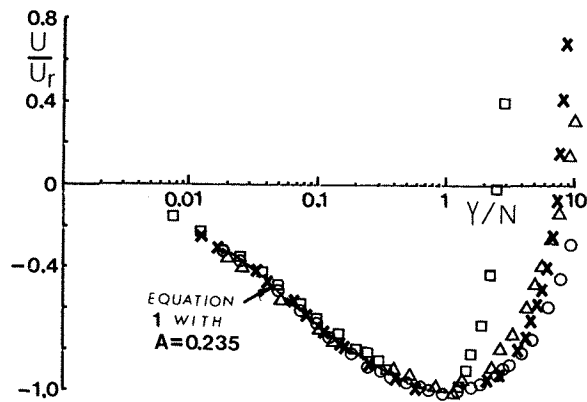


FIGURE 11. Normalised Backflow mean velocity profiles. Legend as in fig.10.

for the boundary layer developing underneath it is that based on the distance from the reattachment point and the minimum (negative) velocity, U_N . Figure 12 shows the values of surface skin friction, also normalised by U_N , plotted against this Reynolds number. Additional data is shown for backward facing step flows (Adams et al¹⁵, Chandrsuda & Bradshaw¹⁶ and Devenport¹⁷) and for the RF flat plate flow, along with some results obtained in our laboratory, also in a normal flat plate flow. The data from all geometries collapse remarkably well. They also lie on a line having a slope of about $-1/2$, consistent with the idea that the boundary layer has strong laminar-like features (see also Adams et al¹⁵). However, we recognise that description of the flow in this region as being essentially laminar is far too simplistic, although there is no doubt that it must be dominated by viscous effects. Perhaps the outer backflow is of such a relatively large scale that it simply acts as a 'quasi-steady' outer boundary condition.

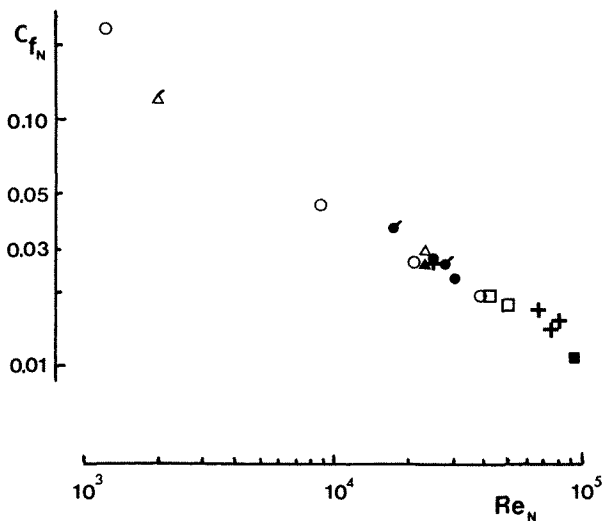


FIGURE 12. Normalised wall friction within separated regions. +, present results. Δ , axisymmetric step, Devenport¹⁷; plane backstep, \blacktriangle , Adams et al¹⁵; \blacksquare , Chandrsuda & Bradshaw¹⁶; normal flat plate; \bullet , Ruderich & Fernholz¹³; \circ , our laboratory. $Re_N = U_N(L_r - x')/\nu$, $C_{fN} = \tau_w/0.5\rho U_N^2$.